Evaluating the structure and magnitude of the ash plume during the initial phase of the 2010 Eyjafjallajökull eruption using lidar observations and NAME simulations

H. F. Dacre,[1] A. L. M. Grant,[1] R. J. Hogan,[1] S. E. Belcher,[1] D. J. Thomson,[2] B. J. Devenish,[2] F. Marenco,[2] M. C. Hort,[2] J. M. Haywood,[2,3] A. Ansmann,[4] I. Mattis,[4] and L. Clarisse[5]

[1] The Eyjafjallajökull volcano in Iceland erupted explosively on 14 April 2010, emitting a plume of ash into the atmosphere. The ash was transported from Iceland toward Europe where mostly cloud-free skies allowed ground-based lidars at Chilbolton in England and Leipzig in Germany to estimate the mass concentration in the ash cloud as it passed overhead. The UK Met Office's Numerical Atmospheric-dispersion Modeling Environment (NAME) has been used to simulate the evolution of the ash cloud from the Eyjafjallajökull volcano during the initial phase of the ash emissions, 14–16 April 2010. NAME captures the timing and sloped structure of the ash layer observed over Leipzig, close to the central axis of the ash cloud. Relatively small errors in the ash cloud position, probably caused by the cumulative effect of errors in the driving meteorology en route, result in a timing error at distances far from the central axis of the ash cloud. Taking the timing error into account, NAME is able to capture the sloped ash layer over the UK. Comparison of the lidar observations and NAME simulations has allowed an estimation of the plume height time series to be made. It is necessary to include in the model input the large variations in plume height in order to accurately predict the ash cloud structure at long range. Quantitative comparison with the mass concentrations at Leipzig and Chilbolton suggest that around 3% of the total emitted mass is transported as far as these sites by small (<100 μm diameter) ash particles.

1. Introduction

[2] On 14 April 2010 the character of eruption at Eyjafjallajökull volcano changed from basaltic lava fountaining to explosive emissions of high levels of ash, causing widespread disruption throughout Europe due to the closure of European airspace. Volcanic ash can cause significant problems for aircraft due to the reduction in visibility, abrasion of aircraft surfaces, and even engine failure [*Casadevall*, 1994; *Guffanti et al.*, 2010]. Thus monitoring and forecasting the dispersion of ash clouds is important for human safety.

[1]Department of Meteorology, University of Reading, Reading, UK.
[2]Met Office, Exeter, UK.
[3]College of Engineering, Mathematics, and Physical Sciences, University of Exeter, Exeter, UK.
[4]Leibniz Institute for Tropospheric Research, Leipzig, Germany.
[5]Spectroscopie de l'Atmosphère, Service de Chimie Quantique et Photophysique, Universitè Libre de Bruxelles, Brussels, Belgium.

[3] The responsibility for issuing advice to aviation about the geographic distribution of volcanic ash from volcanoes are provided by the Volcanic Ash Advisory Centres (VAACs) with responsibility for different regions divided among different operational centers [*Witham et al.*, 2007]. The London VAAC is responsible for ash emitted from volcanoes in Iceland. The UK Met Office's dispersion model, the Numerical Atmospheric-dispersion Modeling Environment (NAME), is used operationally by the London VAAC to forecast the evolution of volcanic ash clouds. The NAME model uses driving meteorology from a numerical weather prediction (NWP) model and input of a number of parameters describing the volcanic source such as plume height, vertical distribution of ash and mass eruption rate [*Leadbetter and Hort*, 2011]. The aim of this paper is to compare NAME simulations of the initial phase of the ash emissions with ground-based lidar observations of ash layers over the UK and Germany with a view to understanding the dispersion of volcanic ash, estimating the plume height at the source, and estimating the distal fine ash fraction which survives the near-source fallout processes. Evaluation of

NAME, using this natural point source release event, will also contribute to improvements in the methods used to simulate the transport and representation of volcanic ash in the model.

[4] In this paper, "plume height" is defined as the maximum height above mean sea level (amsl) that the ash plume reaches in the vicinity of the volcano vent. It is needed as an input to most volcanic ash dispersion models. "Particles" are defined as the entities dispersing in the atmosphere, which may be either unaggregated single grains of ash or aggregates, i.e., clusters of grains of ash. The "distal fine ash fraction" is defined as the fraction of the total emitted mass that is carried by small particles (<100 μm diameter) and transported long distances (of order 1000 km) from the volcano. Large particles, both single large grains and large aggregates, fall out close to the volcano. Aggregation can occur at large distances from the source, e.g., when ash particles are icy or wet [*Durant et al.*, 2009; *Sparks et al.*, 1997], but it is most effective near source. For models which don't represent aggregation processes the distal fine ash fraction is used as a scaling factor that is applied to the model concentrations to allow quantitative predictions of ash quantities at long range.

[5] In this paper the parameters describing the volcanic source are outlined in section 2. A description of the NAME dispersion model and simulations are given in section 3. The lidar observations at Chilbolton in southern England and Leipzig in Germany are described in section 4. A comparison of the lidar and NAME simulated ash cloud over Leipzig and Chilbolton for a constant plume height is given in section 5. Section 6 shows a similar comparison but for a varying plume height. Finally, discussion and conclusions are presented in section 7.

2. Parameters Describing the Effective Volcanic Source

[6] Like many volcanic ash dispersion models, NAME does not represent the complex dynamics which occur close to the volcano and instead assumes an "effective" source describing the injection of material into the atmosphere. The effective source is characterized by several key parameters.

2.1. Plume Height

[7] The height at which ash particles are emitted into the atmosphere at the source has a large influence on the vertical and horizontal structure of the ash plume downstream [*Webley et al.*, 2009]. This is due to the fact that wind speed and direction vary with height and can lead to layering of ash as observed in the radiosonde launch carried out from Stranraer on the 19 April 2010 by *Harrison et al.* [2010] and the lidar observations over Europe [*Ansmann et al.*, 2010; F. Marenco and R. J. Hogan, Determining the contribution of volcanic ash and boundary layer aerosol in backscatter lidar returns: A three-component atmosphere approach, submitted to *Journal of Geophysical Research*, 2011; R. J. Hogan et al., Lidar and Sun-photometer retrievals of ash particle size and mass concentration from the Eyjafjallajökull volcano, manuscript in preparation, 2011]. In order to represent the evolution of the ash cloud accurately, it is necessary to accurately represent the height at which ash particles are emitted.

[8] In this paper, information about the Eyjafjallajökull eruption plume height is taken from measurements provided by the Icelandic Meteorological Office's C-band radar [*Arason et al.*, 2011]. There were time periods when no radar data were available. These periods occurred either because the radar cannot detect the plume when it is below 2.5 km, due to mountain ranges and the curvature of the Earth, or because the plume was obscured by water or ice clouds, or because the radar scan was missing. Furthermore, the maximum observed plume height may not be the maximum height at which ash is injected laterally into the atmosphere. However, for weak eruptions, such as Eyjafjallajökull, the difference is usually less than a few kilometers [*Mastin et al.*, 2009]. In this paper the sensitivity to plume height of the NAME volcanic ash predictions over the UK and Germany is investigated.

2.2. Vertical Distribution of Ash

[9] Information on the lower boundary of the effective source is also difficult to ascertain. In general, by analogy with chimney plumes, one would expect most of the emitted ash from a large-magnitude explosive eruption to be found well above the ground and close to the plume top (in the umbrella cloud) [*Sparks et al.*, 1997]. However, this may not be the case for long-duration eruptions in which plume height is varying and interacting with the background atmosphere, for weak eruptions, or if the plume is collapsing to produce pyroclastic density currents [*Mastin et al.*, 2009; *Bonadonna et al.*, 2002]. Because Eyjafjallajökull was a weak eruption, the minimum height for ash release used in this paper is set to the volcano summit height (1.6 km for Eyjafjallajökull) and ash is assumed to be emitted uniformly (in terms of mass mixing ratio) between the volcano summit and the maximum observed plume height. In an operational context this is a conservative choice which tries to avoid predicting no ash where a significant hazard may exist.

2.3. Mass Eruption Rate

[10] At present there is no direct method of measuring the mass eruption rate of erupting volcanoes. As a result, many VAAC models, including NAME, use empirical relationships to relate observed maximum plume height to the eruption rate [*Wilson et al.*, 1978; *Sparks et al.*, 1997; *Mastin et al.*, 2009]. Details of the relationship used here and comparison with other relationships is included in Appendix A. We note, however, that such relationships have significant uncertainty. In practice, for modeling long-range transport, the important number to quantify is not the total mass eruption rate but the fraction of total emitted mass present in the downstream ash cloud (i.e., carried by small ash particles which do not fall out close to the source). This distal fine ash fraction is used as a scaling factor that is applied to the model amounts to allow quantitative predictions of ash at long range. *Mastin et al.* [2009] provided estimates of the fraction of emitted mass carried by small ash grains (<63 μm diameter) present in the proximal ash deposits that range from 2% to 60% depending on the type of volcano. However, as discussed by *Mastin et al.* [2009], these estimates are based on a wide range of eruption types, some of which generated pyroclastic density currents (producing large volumes of fine ash). As distal ash is often too widely dispersed to be sampled, even though

Table 1. Ash Particle Size Distribution Used in NAME

Particle Diameter (μm)	Fraction of Mass (%)
0.1–0.3	0.1
0.3–1.0	0.5
1.0–3.0	5.0
3.0–10.0	20.0
10.0–30.0	70.0
30.0–100.0	4.4

collectively it is a significant mass, estimates of the overall grain size distribution are frequently based on an analysis of the grain size distribution of deposits close to the volcano such as that by Mastin et al. However, this may underestimate the overall fraction of fine ash grains [*Bonadonna and Houghton*, 2005]. In addition such measurements refer to grain size and so, all else being equal, will tend to overestimate the fraction of fine particles if there is significant aggregation. An estimation of the distal fine ash fraction for the initial phase of the eruption using a novel method based on modelled and remotely sensed observations of ash concentration is made in this paper.

2.4. Size Distribution of Ash

[11] All of the emitted mass in NAME is distributed among particles with a diameter drawn from the size distribution shown in Table 1. This distribution is based on an average of measurements made in the plumes from explosive eruptions of Mount Redoubt on 8 January 1990, Mount St Helens on 18 May 1980, and St Augustine on 8 February

1976 [*Hobbs et al.*, 1991; *Leadbetter and Hort*, 2011]. Ash density in NAME is assumed to be 2300 kg m^{-3}.

3. NAME Simulations

[12] NAME is a Lagrangian particle trajectory model designed for many dispersion applications, including the prediction of the dispersion and deposition of volcanic ash in the atmosphere [*Jones et al.*, 2007]. Emission of volcanic ash is modelled by releasing ash particles into the model atmosphere (120,000 particles/h for the simulations in this paper), with each model particle representing a mass of volcanic ash. The model ash particles are carried along by the wind with turbulent mixing represented by giving the trajectories a stochastic perturbation using semiempirical turbulence profiles. NAME also includes treatments of sedimentation and dry and wet deposition. The sedimentation uses a fall velocity calculated using the Reynolds number dependent drag coefficient given by *Maryon et al.* [1999] with the Cunningham correction applied for small particle sizes. The dry deposition parametrization uses a deposition velocity calculated by the resistance analogy and is combined with the sedimentation as described by *Webster and Thomson* [2008]. Wet deposition uses scavenging coefficients and accounts for rain out and wash out by precipitation as described by *Maryon et al.* [1999].

[13] In this paper, NAME III (version 5.4) is driven using the 3-D winds and thermodynamic fields from UK Met Office global NWP model analysis fields, updated every 6 h and forecast fields updated every 3 h. Ash concentrations are computed by summing the mass of ash
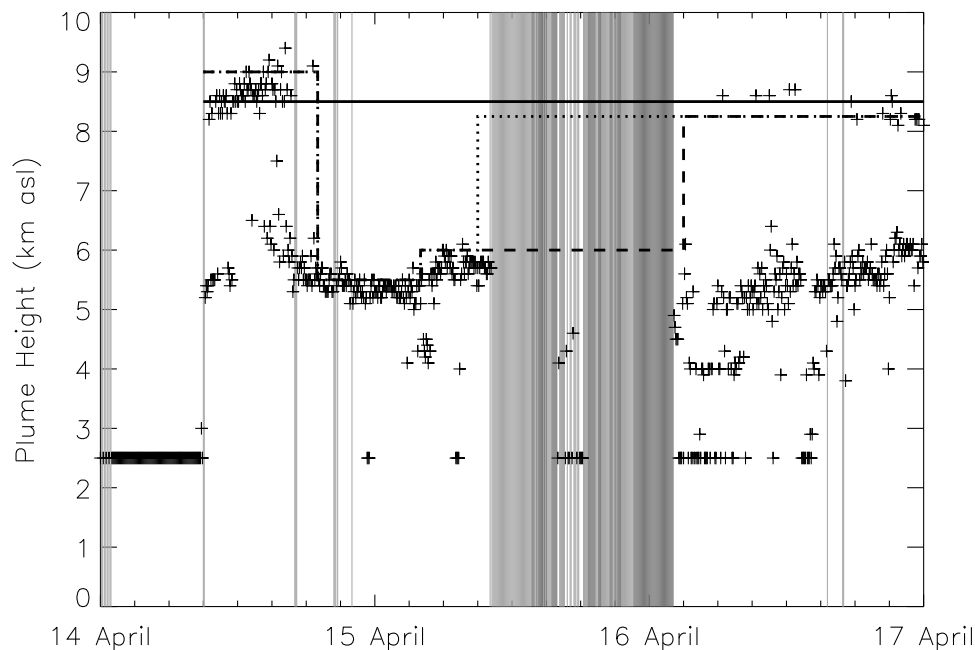

Figure 1. Five minute time series of plume height from the Icelandic radar (crosses), for the constant plume height simulation (solid line), low plume height reconstruction (dashed line), and high plume height reconstruction (dotted line). The grey area represents missing radar data due to missing scans (light grey) or clouds (dark grey). The minimum plume height detectable due to mountain ranges and curvature of the Earth is 2.5 km. Where no plume is detected (but radar data is not missing), 2.5 km has been plotted.
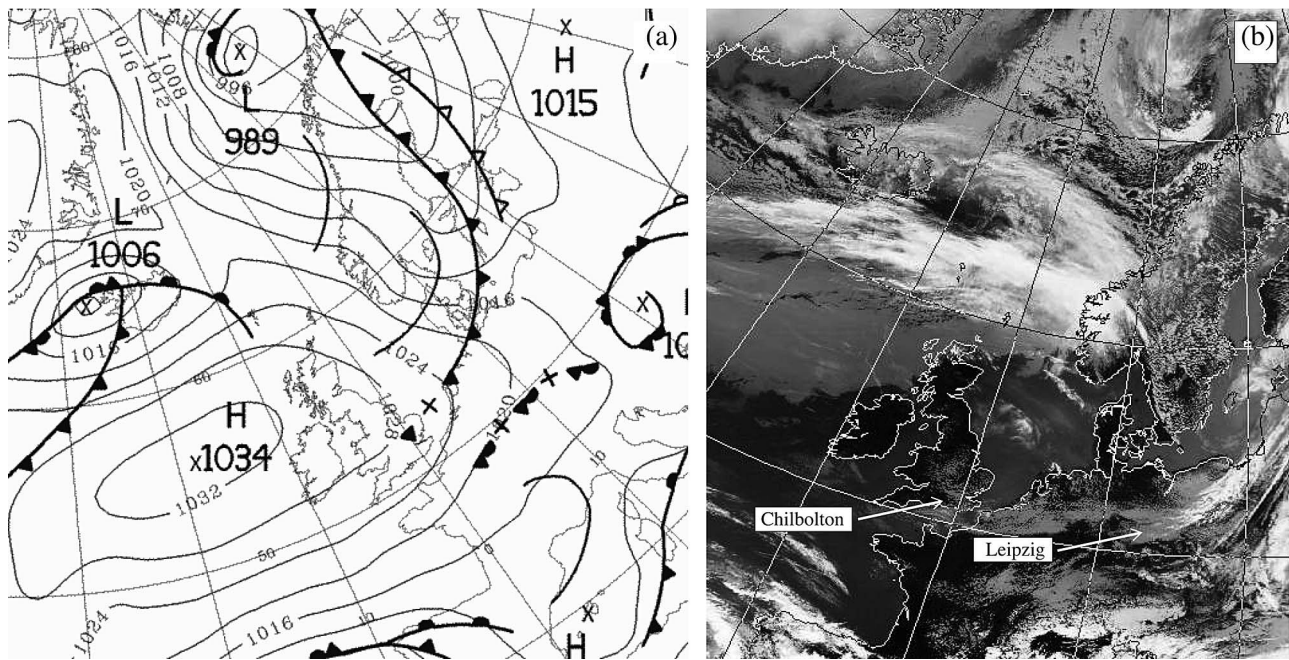
Figure 2. (a) Synoptic analysis at 00:00 UTC on 16 April 2010 from the UK Met Office. (b) AVHRR thermal infrared image (11.5–12.5 μm) at 12:55 UTC on 16 April 2010 courtesy of Dundee satellite receiving station.

particles in areas of 0.375° latitude by 0.5625° longitude (approximately 40 km × 40 km), averaged over 200 m in the vertical and over a time period of 1 h.

[14] Plume height input is taken from measurements provided by the Icelandic Meteorological Office's C-band radar [*Arason et al.*, 2011] (http://andvari.vedur.is/~arason/radar/). Figure 1 shows the 5 min time series of plume height from the Icelandic radar. It is clear that the plume height from the radar varies on a range of timescales from minutes to hours. The grey shading represents missing radar data due to missing scans or clouds obscuring the ash plume; 89.4% of the data is missing between 09:00 UTC on 15 April and 03:00 UTC on 16 April, 46.3% due to missing scans, 36.6% due to cloud obscuring the ash plume, and 6.5% due to plume height below 2.5 km. The authors are not aware of any observations available to verify the plume height during this time. Therefore in this paper three simulations of the Eyjafjallajökull volcano ash dispersion have been performed with different plume height input. For our control simulation a constant plume height of 8.5 km amsl was used for the first 96 h of the simulation which began at 09:00 UTC on 14 April 2010. The second and third simulations used a varying plume height that represents the varying plume height detected by the radar in Iceland. Note that plume height variations are represented on timescales of 6 h or more. No attempt has been made to follow every fluctuation in the radar data. Values of plume height have been chosen to pass through the upper end of the scatter in the 5 min radar values while not reflecting the most extreme values. For the period in which few radar observations were available, two reconstructions are made. In the first reconstruction the plume height is kept constant at 6 km from 09:00 UTC on 15 April until

03:00 UTC on 16 April at which point it is increased to 8.25 km, referred to in this paper as the low plume height reconstruction. In the second reconstruction the plume height is increased immediately from 6 km to 8.25 km amsl at 09:00 UTC on 15 April and then kept constant, referred to in this paper as the high plume height reconstruction. These reconstructions represent the uncertainty in the plume height input. For all three simulations ash was emitted uniformly between the volcano summit and the plume height.

4. Observations

[15] From the 14–16 April 2010 a high-pressure system was located over the UK and the north Atlantic and a low-pressure system was located over northern Europe (Figure 2a) resulting in the ash cloud being transported to the southeast. A decaying cold front associated with the low-pressure system was moving southwards over the UK. Mostly cloud-free skies over much of Europe during this period (Figure 2b) allowed the ash cloud to be observed by several ground based lidars. Two such lidar retrievals were obtained at Chilbolton, in the south of England (51.1°N, 1.4°W), and at Leipzig in Germany (51.4°N, 12.4°E) on 16 April 2010.

4.1. Chilbolton Lidar

[16] Figure 3a shows the range-corrected lidar backscatter from the ground-based lidar at Chilbolton on 16 April 2010. The ash cloud was first observed over Chilbolton at a height of 3 km at 12:00 UTC on 16 April 2010. The height of the ash cloud decreased with time and intercepted the boundary
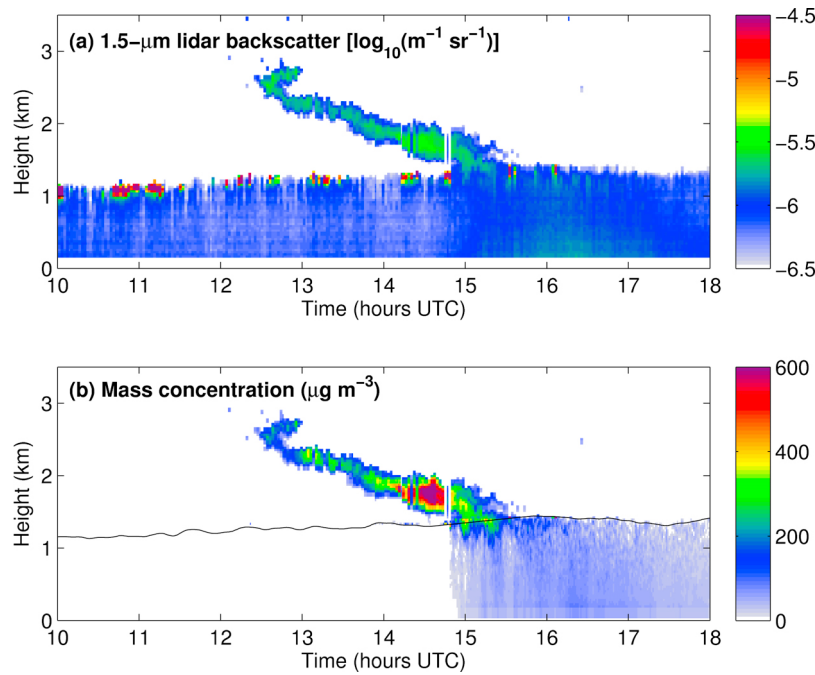
Figure 3. Time-height plots at Chilbolton (51.1°N, 1.4°W) from 10:00 to 18:00 UTC on 16 April 2010. (a) Lidar backscatter and (b) mass concentration retrieved from a combination of lidar and Sun photometer measurements overlaid with the boundary layer top (black line).

layer at 15:00 UTC. The "effective thickness" of the layer, defined as the total column mass divided by the peak mass concentration, was approximately 500 m. Figure 3b shows the ash mass concentrations derived by Hogan et al. (manuscript in preparation, 2011) from a combination of the ground-based lidar and Sun photometer measurements overlaid with the boundary layer top. The boundary layer top is estimated as the height at which the 1.5 μm lidar backscatter signal is no longer significant (Figure 3a). For the period during which the ash cloud intersects the top of the boundary layer, 15:00–15:30 UTC, the boundary layer height has been interpolated. The peak mass concentrations of 690 ± 210 μg m^{-3} were retrieved at 14:34 UTC at a height of 1.7 km above the surface. Similar sloping ash plumes and concentrations were observed over Exeter on 16 April (Marenco and Hogan, submitted manuscript, 2011).

4.2. Leipzig Lidar

[17] *Ansmann et al.* [2010] also observed an ash cloud using the ground-based lidar at Leipzig on 16 April 2010 [*Ansmann et al.*, 2010, Figure 1]. The lidar observations at Leipzig were largely obscured by low-level cloud between 05:00 and 12:00 UTC on 16 April 2010 although ash was observed for a short time at 09:20 UTC, at a height of 5 to 7 km. From 12:00 to 18:00 UTC the base of the ash cloud decreased with time, as at Chilbolton, descending from 5 to 2 km. The ash cloud over Leipzig had an effective thickness of approximately 1 km with peak mass concentrations of 1000 μg m^{-3} retrieved between 12:00 and 13:00 UTC at a height of 3.2 km above the surface. The descent of the ash cloud is not the result of a descending ash layer but is due to the advection of a sloping structure over Leipzig.

This sloping structure was observed by NASA's Cloud-Aerosol Lidar and Infrared Pathfinder Satellite Observations (CALIPSO) satellite which captured an image of the volcanic ash cloud on 17 April as it drifted over Europe (http://atrain.nasa.gov/stories.php).

5. Constant Plume Height

[18] In this section the NAME simulation of the initial phase of the eruption (14–16 April), using a constant plume height of 8.5 km amsl (control simulation), is summarized and compared with the observed ash cloud over Leipzig and Chilbolton.

5.1. Summary of Initial Phase of Eruption

[19] Figure 4 shows maps of column-integrated mass concentration obtained from the NAME control simulation for the initial phase of the eruption. It should be noted that the impression given in comparing observed and NAME-simulated ash concentration can be dependent on the contour interval chosen for plotting both the observed and modeled ash concentrations. In this paper NAME mass concentrations are plotted on a linear scale but an outline of the outermost extent of the simulated ash cloud is also plotted. The shaded part of the plume at 00:00 UTC on 15 April (Figure 4a) contains 96% of the mass, the fraction reduces to 75% at 12:00 UTC on 16 April (Figure 4d). An arbitrary scale is used to avoid implying quantitative predictions of ash concentrations at long-range where the distal fine ash fraction is not known.

[20] Initially, the NAME simulated ash cloud was advected southeastward from Iceland toward western Europe (Figure 4a). After 24 h the ash cloud began to diverge and
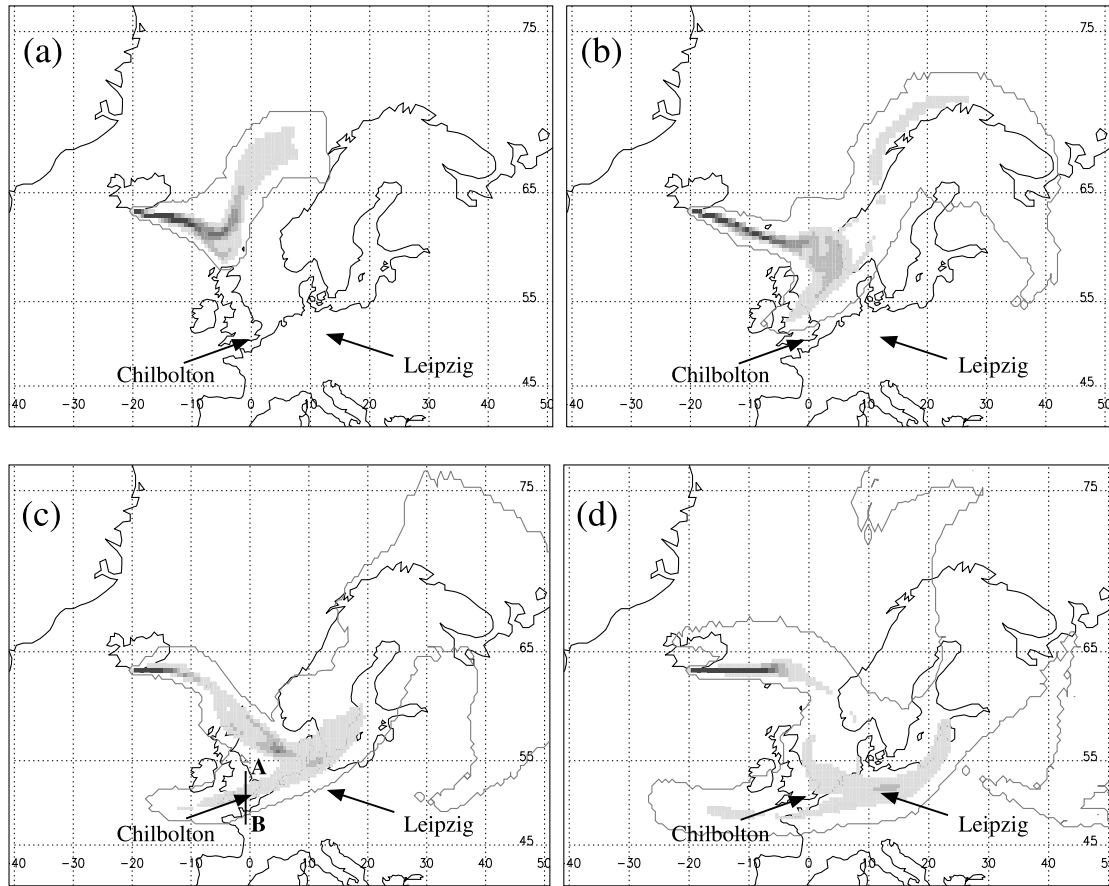
Figure 4. Column-integrated NAME mass concentration from the control simulation at (a) 00:00 UTC on 15 April 2010, (b) 12:00 UTC on 15 April 2010, (c) 00:00 UTC on 16 April 2010, and (d) 12:00 UTC on 16 April 2010. The shaded concentration contours are in arbitrary units, contours are equally spaced concentration levels, and span a factor of 5 across the entire range of levels. The grey line outlines the outermost extent of the ash cloud. The black line, AB, indicates the location of the vertical cross section in Figure 5.

transport occurred both northeastward and southwestward, parallel to the cold front associated with the low-pressure system over Scandinavia (Figure 2a). A branch of the ash cloud was advected over the UK (Figure 4b) reaching Chilbolton (51.1°N, 1.4°W) at 17:00 UTC on 15 April 2010 (Figure 4c).

[21] Figure 5 shows a vertical cross section through the branch of the ash cloud that was forecast to be advected over the UK at 00:00 UTC on 16 April 2010 (along the line AB in Figure 4c). The ash layer has a sloping structure that extends from 6 km to the surface. As with Leipzig, the descending base of the ash cloud observed over Chilbolton
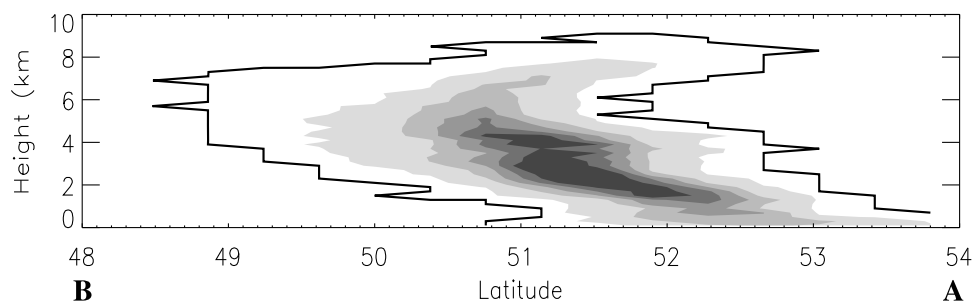

Figure 5. Vertical cross section of mass concentration from 48°–54°N at 1.4°W (along line, AB, in Figure 4c). The shaded concentration contours are in arbitrary units, contours are equally spaced concentration levels and span a factor of 5. The black contour outlines the outermost extent of the ash cloud.

Table 2. Volcanic Ash Over Cardington, Reading, Chilbolton, and Exeter Observed by Ground-Based Lidars and NAME Volcanic Ash Between 1.2 and 12 km and Between 1.2 and 3.2 km[a]

Location	Lat/Lon (°N, °W)	Model/Observation	15 April 2010 (UTC)																	16 April 2010 (UTC)													
			15	16	17	18	19	20	21	22	23	00	01	02	03	04	05	06	07	08	09	10	11	12	13	14	15	16	17	18	19	20	21
Cardington	52.1, 0.4	NAME	N1	N1	N1	N1	N1	N2	N2	N2	N2	N2	N2	N2	N2	N2	N2	N2	N2	va	va	va	va	va	va	va							
		Lidar																							va	va							
Reading	51.3, 0.6	NAME		N1	N1	N1	N2	N2	N2	N2	N2	N2	N2	N2	N2	N2	N2	N2	N2	va	va	va	va	va	va	va							
		Lidar																					va	va	va							
Chilbolton	51.1, 1.4	NAME			N1	N1	N1	N2	N2	N2	N2	N2	N2	N2	N2	N2	N2	N2	N2	N2	N2	N2	va	va	va	va							
		Lidar																								va	va						
Exeter	50.7, 3.5	NAME				N1	N1	N1	N1	N2	N2	N2	N2	N2	N2	N2	N2	N2	N2	N2	N2	N2	N2	N2	N2	N2	va						
		Lidar																							va	va	va	va	va	va	va	va	va	va

[a]Abbreviations: va, volcanic ash; N1, NAME volcanic ash between 1.2 and 12 km; and N2, NAME volcanic ash between 1.2 and 3.2 km only. UTC times are hours; for example, 15 denotes 15:00.

(Figure 3) and the other UK lidars is the result of advection of a sloping structure over the sites and is not a result of a descending ash layer.

[22] Table 2 shows the time at which volcanic ash was observed by ground-based lidars at Cardington, Reading, Chilbolton, and Exeter in the UK (locations are shown in Figure 6) as well as the time at which significant ash is present in the model at these locations. As the volcanic ash detection limit for each lidar is not known, it is not possible to set an equivalent threshold for ash concentrations in NAME. Therefore, in Table 2, significant modelled ash concentration thresholds are defined as ash concentrations that are >1% of the peak concentration predicted over each lidar location. The presence of significant ash concentrations over the four UK lidar locations in NAME has been determined for two layers of the atmosphere, between 1.2 and 12 km above the surface and between 1.2 and 3.2 km above the surface. The first layer encompasses the whole depth of the NAME simulated ash cloud as it passed over the UK and the second layer encompasses the depth of the atmosphere in which volcanic ash cloud was actually observed by the lidars in the UK. It is evident that a timing error exists between the NAME simulations and the observed ash at all of the UK lidar sites.

[23] The NAME simulated ash travels southward over the UK on 15 and 16 April with a southward velocity of ≈6 ms^{-1} in the east of the UK and ≈4 ms^{-1} in the west of the UK. The mean wind speed between 1.2 and 3.2 km measured by the 09:00 UTC 16 April radiosonde at Larkhill (51.2°N,1.8°W) was 9.7 ms^{-1} with a mean wind direction in the same layer of 51.8°, giving a southward wind velocity of 6.0 ms^{-1}. This is consistent with the NAME simulated ash cloud propagation speed therefore the timing difference between the NAME simulation and the observed ash cloud over Chilbolton is unlikely to be due to an incorrect propagation speed. However, Figure 6 shows the MODIS AQUA visible satellite image at 13:23 UTC on 16 April. An east–west orientated band of volcanic ash can be seen stretching from southern England to Belgium over the English Channel. The feature to the north is an algal bloom or sediment and can be distinguished from the ash cloud as it remains stationary while the ash cloud travels southward. The location of this ash cloud corresponds well with the NAME simulated ash cloud at 00:00 UTC on 16 April (Figure 4c). This suggests that the timing difference between the NAME simulation and the observed ash cloud over Chilbolton is caused by cumulative errors in the driving NWP wind fields used in NAME resulting in a positional error in the north–south direction of around 200 km.

[24] Figure 7 shows the ash cloud and its initial transport as measured by the Infrared Atmospheric Sounding Interferometer (IASI) on board METOP-A. Infrared sounders are very sensitive to the presence of minerals [*Clarisse et al.*, 2010a]. Volcanic ash in particular has a very specific infrared signature [*Holasek and Rose*, 1991; *Schneider and Rose*, 1994; *Gangale et al.*, 2010], which makes it differentiable from other aerosols and clouds. The specific ash signature depends on the mineral composition and the particle size distribution of the ash and a general and robust method for detecting ash from high-resolution infrared sounders was recently proposed by *Clarisse et al.* [2010b].
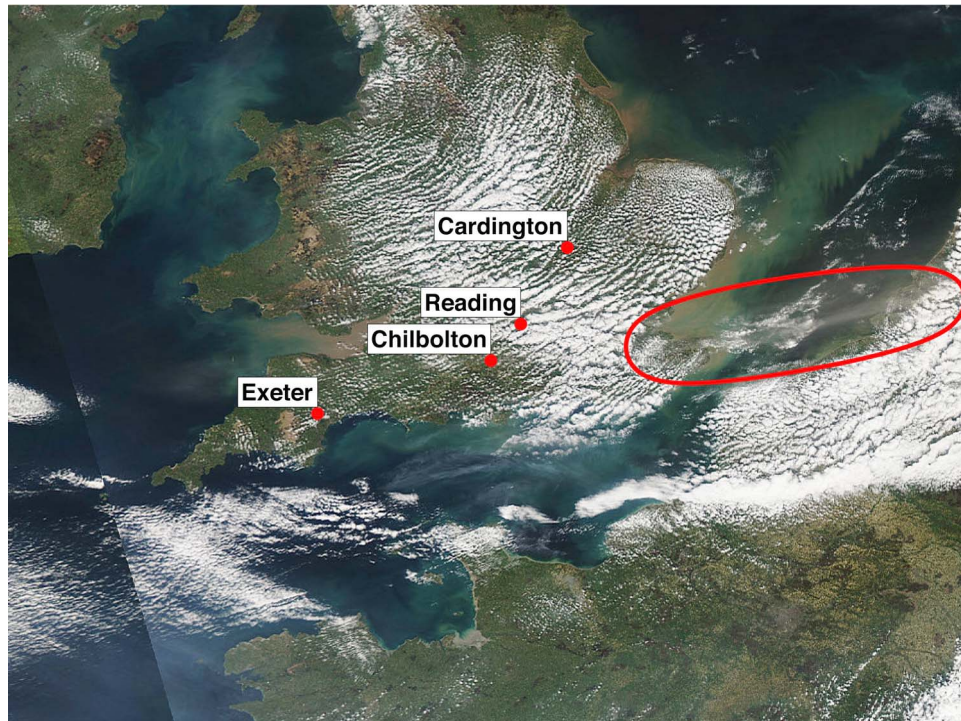
Figure 6. MODIS AQUA visible image at 13:23 UTC on 16 April showing a volcanic ash cloud (enclosed by the red contour) stretching from southern England to Belgium. The locations of the UK lidars at Cardington, Reading, Chilbolton, and Exeter are overlaid.
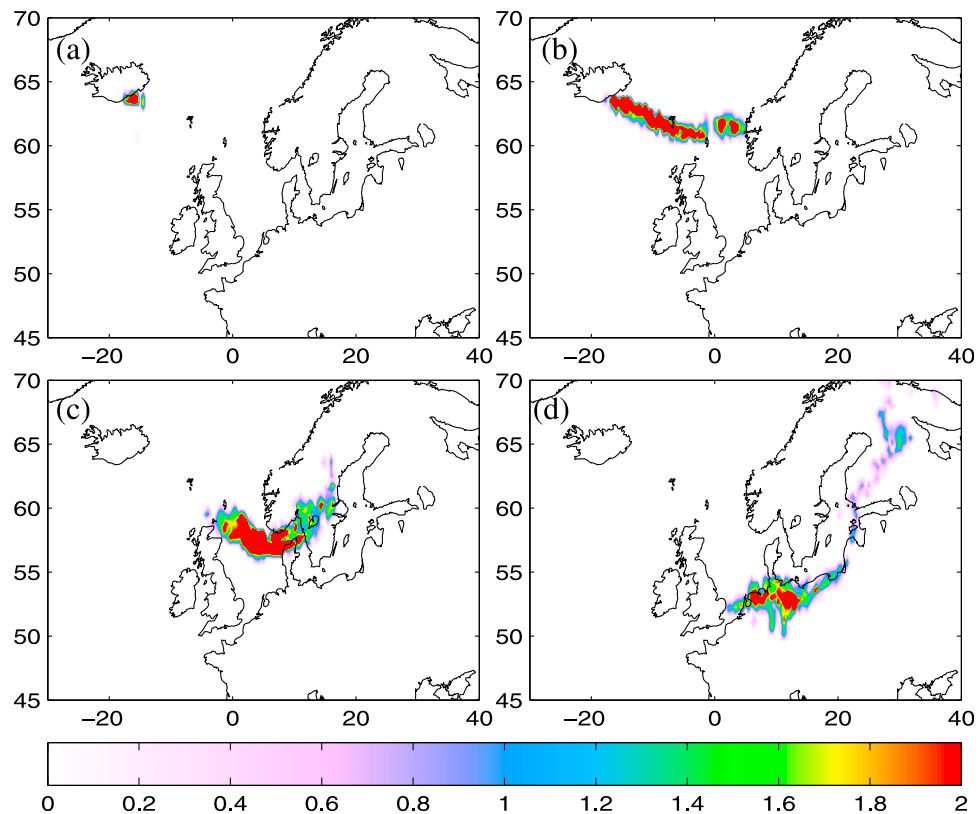

Figure 7. IASI measured volcanic ash index (K) at (a) 22:00 UTC on 14 April 2010, (b) 10:00 UTC on 15 April 2010, (c) 22:00 UTC on 15 April 2010, and (d) 10:00 UTC on 16 April 2010.
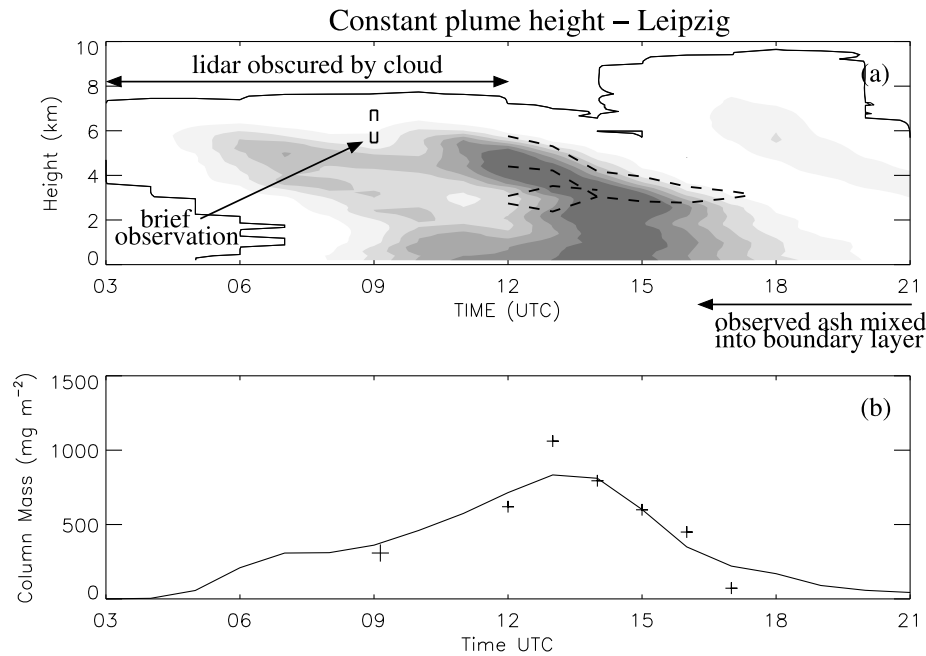
Figure 8. Constant plume height simulation on 16 April 2010. (a) Time-height plot of NAME mass concentration over Leipzig (51.4°N, 12.4°E) on 16 April 2010 overlaid with the outline of the lidar ash cloud (dashed line). The shaded concentration contours are in arbitrary units, contours are equally spaced concentration levels and span a factor of 6. The solid black contour outlines the outermost extent of the modeled ash cloud. (b) Time series of above boundary layer integrated mass loading over Leipzig, from NAME (solid line) and the lidar retrieval (crosses).

We have applied the method here on the first four IASI overpasses after the eruption and the result is shown in Figure 7. Measurements have been quantified using an ash absorption index (brightness temperature difference between 1168 cm^{-1} and 1231.5 cm^{-1}) for measurements which pass the ash detection test (and 0 for those that do not).

[25] In the NAME simulation Leipzig is close to the central axis of the ash cloud and ash was transported over Leipzig at 05:00 UTC on 16 April (Figure 4d). Figure 7 shows the ash measured by IASI. The ash cloud does not show up in it's entirety due to the detection limits of the instrument and the presence of cloud. However, the spatial correlation of the IASI ash cloud and the highest concentrations in the main part of the NAME cloud (Figures 4a–4d) is remarkably good, particularly over Leipzig (Figures 4d and 7d), suggesting that NAME correctly predicts the time of arrival of the ash cloud at the central axis over Leipzig.

5.2. Constant Plume Height: Leipzig

[26] Figure 8a shows NAME mass concentration results for Leipzig with the outline of the lidar ash cloud overlaid. Note that the lidar observations at Leipzig were largely obscured by low-level cloud between 05:00 and 12:00 UTC on 16 April 2010. Ash was briefly detected at 09:00 UTC in a layer between 5 and 7 km. NAME shows significant amounts of ash arriving over Leipzig at 05:00 UTC, with the top of the ash cloud at 6 km, and maximum mass concentrations centered at 5 km. Between 12:00 and 15:00 UTC NAME captures the sloping upper ash layer seen by the lidar although in NAME the layer appears to be about 500 m

lower than the observed layer and toward the end of this period, the NAME ash cloud extends to the ground. Mixing of ash into the boundary layer is also observed by *Ansmann et al.* [2010] after 16:00 UTC. The ash layer centered at 3 km seen in the lidar observations after 12:00 UTC is not apparent in NAME but NAME shows an increase in ash concentration below 3 km.

[27] Figure 8b compares time series of the column-integrated mass loading derived from NAME and the Leipzig lidar measurements. The lidar mass loadings have been calculated by integrating from the top of the boundary layer upward as the *Ansmann et al.* [2010] measurements include backscatter from boundary layer aerosol while the NAME mass loadings are calculated by integrating from 1.2 km upward. The quantitative agreement between NAME and the lidar observations is obtained by assuming that the distal fine ash fraction is 1.5%, i.e., the NAME mass concentrations match the observed concentrations if the modeled concentrations are scaled by 1.5%. This suggests that 98.5% of the emitted mass falls out close to the source. There are of course uncertainties in this estimate arising from inaccuracies in the modeling (including any inaccuracies in the mass emission rate). The distal fine ash fraction is assumed to be constant with time.

5.3. Constant Plume Height: Chilbolton

[28] Figure 9a shows the NAME results for Chilbolton with the outline of the lidar ash cloud overlaid. The NAME simulation shows a layer of ash with a sloping structure extending between 6 km and 1 km. A hook-like feature is
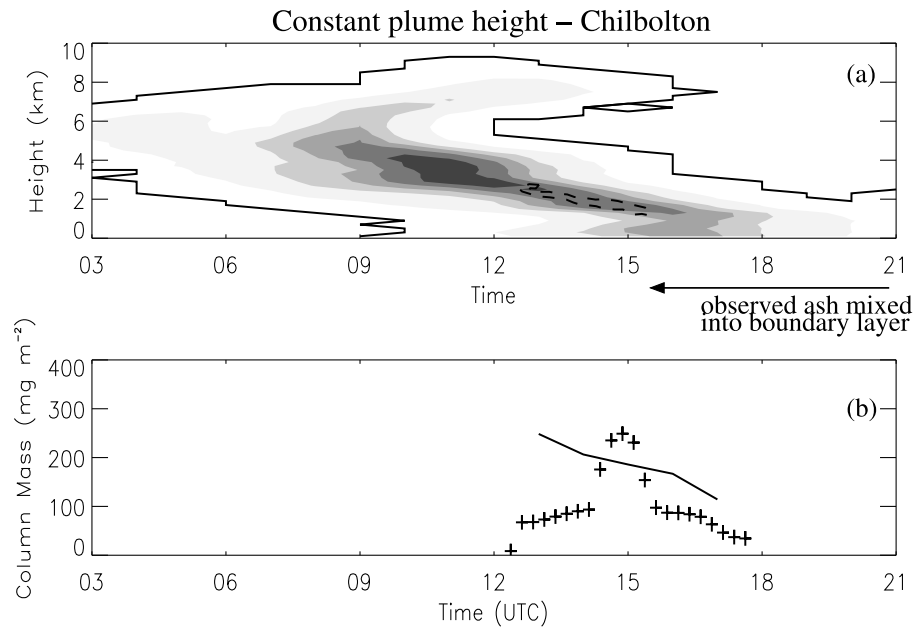
Constant plume height – Chilbolton

Figure 9. Constant plume height simulation on 16 April 2010. (a) Time-height plot of mass concentration over Chilbolton (51.1°N, 1.4°W) on 16 April 2010 overlaid with the outline of the lidar ash cloud (dashed line). The NAME results have been shifted by 9 h so that the vertical structure of the NAME ash cloud and the observed ash cloud coincide. The shaded concentration contours are in arbitrary units, contours are equally spaced concentration levels and span a factor of 5. The solid black contour outlines the outermost extent of the modeled ash cloud. (b) Time series of above boundary layer integrated mass loading over Chilbolton, from NAME (solid) and the lidar retrieval (crosses). NAME column-integrated mass loading are only plotted for the time during which the NAME and lidar observations match.

also seen in the NAME simulation from 6 km to 8 km bending back over the top of the sloping structure. As discussed in section 5.1, in NAME the ash cloud arrives earlier than was observed over Chilbolton. Therefore for this comparison the NAME ash cloud has been shifted into the future by 9 h so that the sloped structure of the NAME ash cloud and the observed ash cloud coincide. A shift of 9 h is assumed for the Chilbolton ash cloud for the remainder of this paper. This shift is consistent with the observations from other UK lidars in Exeter, Cardington and Reading (see Table 2). Between 13:00 and 17:00 UTC NAME captures the sloped ash layer seen by the lidar, although the NAME layer has an effective thickness of approximately 2 km compared to an observed ash cloud effective thickness of 500 m. Earlier NAME shows significant amounts of ash arriving at Chilbolton between 4 and 8 km which was not observed by any of the 4 UK lidars that detected ash. Potential causes of this difference are discussed in section 6.

[29] Figure 9b shows estimates of the column integrated ash derived from the Chilbolton lidar measurements (Hogan et al., manuscript in preparation, 2011) compared with those calculated from NAME for the period during which the NAME and lidar observations match, i.e., between 13:00 and 17:00 UTC only. The lidar and NAME mass loadings have been calculated by integrating from the surface. The quantitative agreement between NAME and the lidar ob-

servations is obtained by assuming a distal fine ash fraction of 2%. This is a similar scaling used to gain quantitative agreement between the NAME simulations and the Leipzig lidar and for the lidar at Exeter (Marenco and Hogan, submitted manuscript, 2011; B. J. Devenish et al., A study of the arrival over the United Kingdom in April 2010 of the Eyjafjallajökull ash cloud using ground-based lidar and numerical simulations, submitted to *Atmospheric Environment*, 2011). Thus it appears that using a constant plume height NAME is able to capture the structure and timing of the ash cloud over Leipzig but, although the sloped structure of the ash cloud is captured over Chilbolton, the upper-level ash and the timing of the ash cloud does not agree with the UK lidar observations.

6. Varying Plume Height

[30] In this section we investigate the potential causes of the NAME overprediction of ash between 4 and 8 km over Chilbolton. One potential explanation is missing processes in NAME such as increased fall speed due to accretion of ice/water on to ash particles and/or aggregation. During the initial phreatomagmatic phase of the eruption, significant cirrus cloud was generated. Ice crystal growth on ash particles followed by turbulence or fall-speed induced aggregation, wet aggregation (as the ash hydrometeors pass through the melting level [*Durant et al.*, 2009; *Folch et al.*, 2010]),
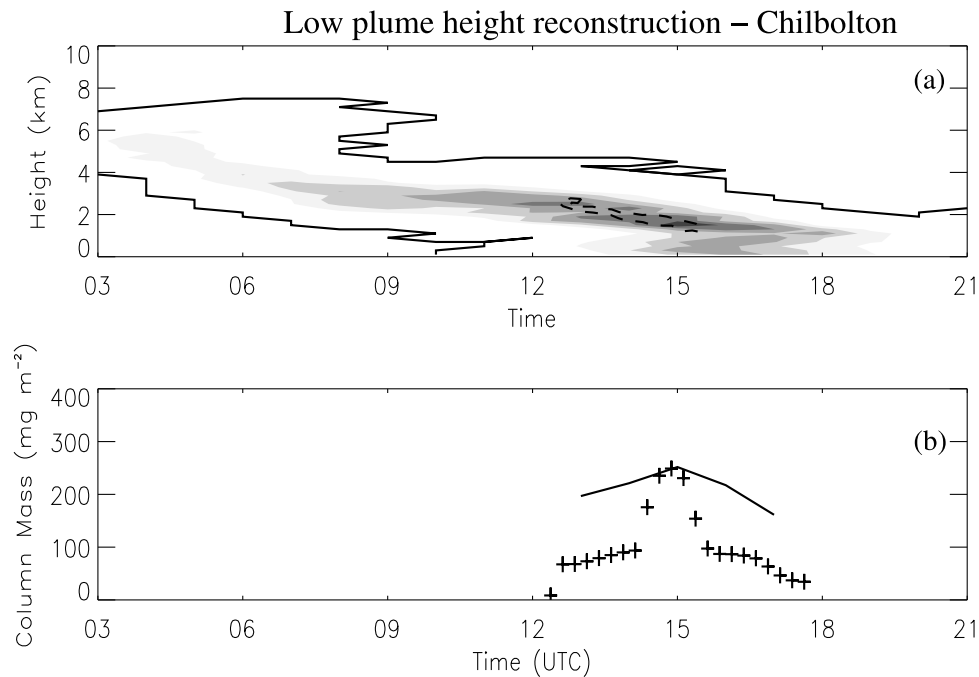
Low plume height reconstruction – Chilbolton

Figure 10. Same as Figure 9 but for low plume height reconstruction simulation over Chilbolton.

and increased electrostatic binding of ash [*James et al.*, 2002; *Harrison et al.*, 2010] can result in rapid aggregate fallout due to increased sedimentation. Thus aggregation processes significantly reduce the proximal fine ash fraction and alter the effective particle size distribution. Although aggregation is most effective near the source, aggregation of small grains can also occur at large distances from the source, due to the interaction of ash with ice or water. Aggregation processes occurring in the distal ash cloud are not represented in NAME. However, *Rose et al.* [2000] and *Folch et al.* [2010] show that the effect of aggregation in the distal ash cloud is likely to be small. Thus it is unlikely that missing aggregation processes in the distal ash cloud can explain the over-prediction of ash between 4 and 8 km over Chilbolton.

[31] Another potential cause of the NAME over-prediction of ash between 4 and 8 km over Chilbolton could be that errors in the driving wind fields led to upper-level ash being transported in the wrong direction particularly at the complex divergence point on the cold front. In this case, the upper-level ash transported over Chilbolton in NAME would have been transported over mainland Europe instead. However, the CALIPSO satellite image on 17 April taken over mainland Europe does not show ash higher than 5.5 km amsl.

[32] Other potential causes of the NAME overprediction of ash between 4 and 8 km over Chilbolton are the failure in our control simulation to represent the variations in plume height that were observed in the early phase of the eruption (Figure 1) and the potential difference between the maximum observed plume height and the maximum height at which ash was injected laterally into the atmosphere. It is quite likely that a constant plume height of 8.5 km, used in the NAME simulation in section 5, overestimates the actual

plume height at the time at which ash contributing to the Chilbolton ash cloud was emitted.

[33] Simulations have been performed in which a time varying plume height was used to determine the impact of variations in plume height on long-range volcanic ash predictions. The plume height estimates have been obtained from the Icelandic radar. Where radar observations are mostly missing (09:00 UTC on 15 April to 03:00 UTC on 16 April) two reconstructions have been made. In the first reconstruction the plume height was kept constant at 6 km (low plume height reconstruction). In the second reconstruction the plume height was kept constant at 8.25 km (high plume height reconstruction).

6.1. Low Plume Height Reconstruction: Chilbolton

[34] Figure 10a shows the mass concentration over Chilbolton for the low plume height reconstruction simulation. Varying the plume height affects both the maximum ash cloud depth and the mass concentrations of the simulated ash cloud over Chilbolton. Compared to the constant plume height simulation (Figure 9a), the maximum ash cloud depth has decreased by 3 km. The vertical distribution of ash now agrees better with the Chilbolton lidar observations. The magnitude of the mass concentrations also reduces as the plume height reduces (due to equation (1), in Appendix A). In order to agree with the estimated column loadings from the lidar observations (Figure 10b) the distal fine ash fraction has been increased from 2% to 3%.

6.2. Low Plume Height Reconstruction: Leipzig

[35] Figure 11a shows the NAME ash cloud at Leipzig for the low plume height reconstruction simulation. The upper-layer of ash observed in the lidar observations after
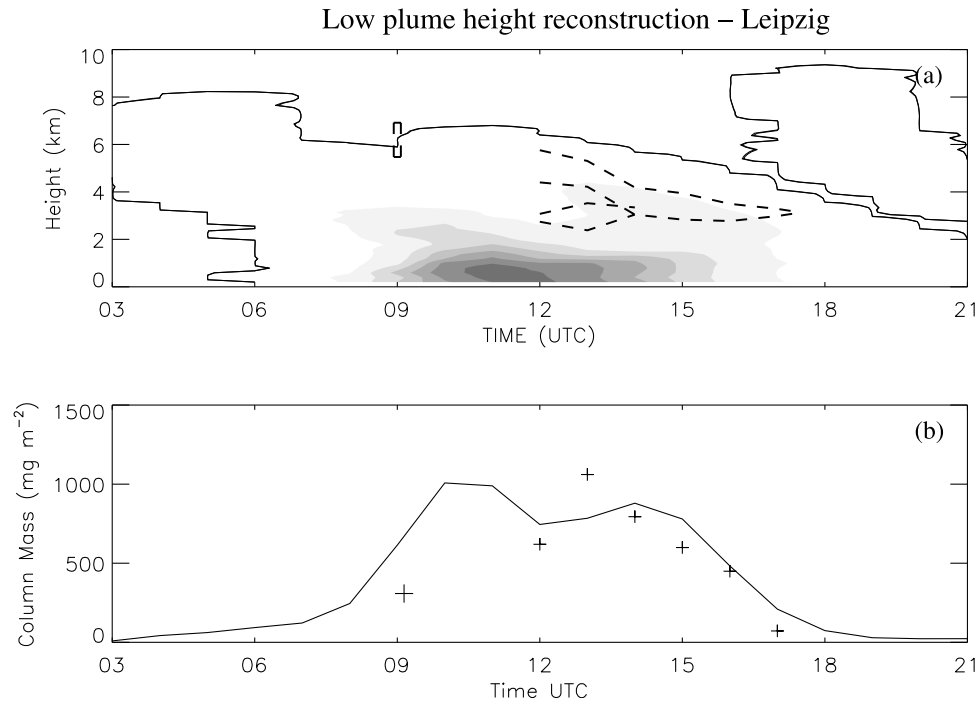
Low plume height reconstruction – Leipzig

Figure 11. Same as Figure 8 but for low plume height reconstruction simulation over Leipzig.

12:00 UTC on 16 April and the early arrival of the ash cloud between 5 and 7 km at 09:00 UTC are now not predicted by NAME. Thus using the low plume height reconstruction produces a prediction that does not agree as well as the constant plume height prediction over Leipzig. In addition, the distal fine ash fraction estimated from the column loadings (Figure 11b) would need to be increased from 1.5% to 10%. Thus the NAME simulation and the

Leipzig lidar observations are more consistent when emission is spread throughout the column over a range of heights up to 8.5 km amsl.

6.3. Mean Emission Time

[36] In order to determine whether or not ash emitted at the same time contributed to the ash observed at both Chilbolton and Leipzig the mean emission time of the
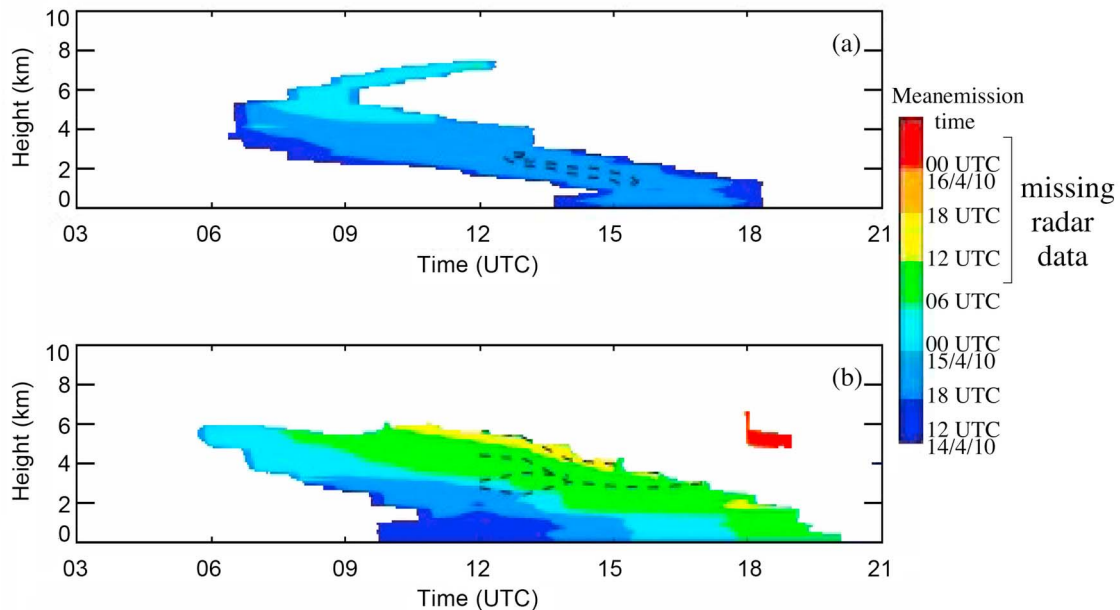

Figure 12. Time-height plots of mean emission time on 16 April 2010 at (a) Chilbolton and (b) Leipzig for the constant plume height simulation.

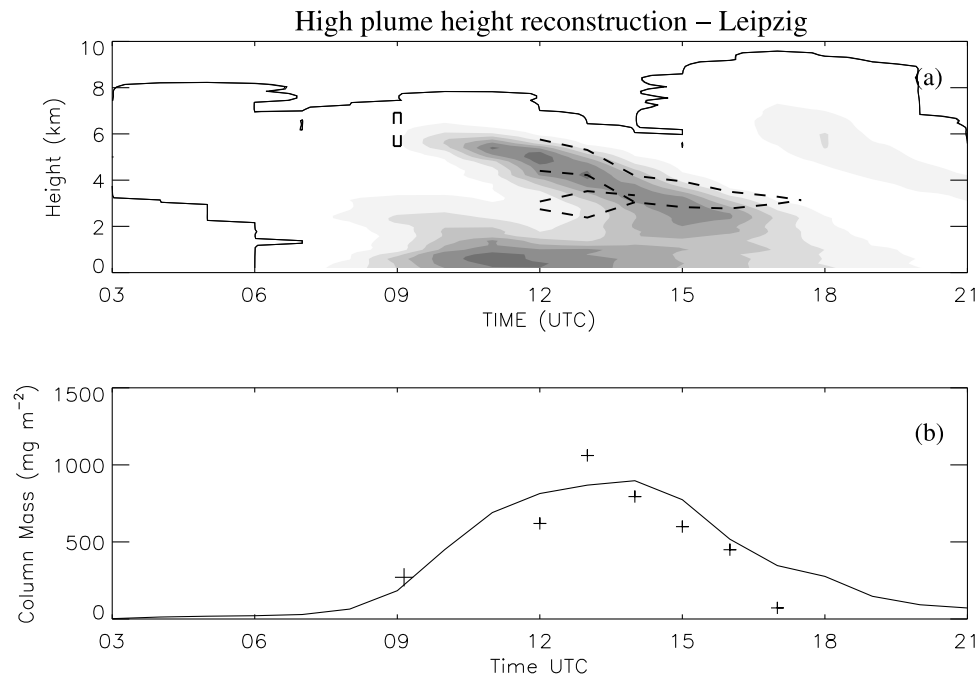High plume height reconstruction – Leipzig

Figure 13. Same as Figure 8 but for high plume height reconstruction simulation over Leipzig.

material contributing to each concentration estimate has been estimated (for the constant plume height case). The "mean emission time" is defined as the mean time at which ash particles contributing to the concentration in a volume of the atmosphere are emitted from the volcano. In these NAME simulations the volume of the atmosphere is approximately 40 km × 40 km in the horizontal and 200 m in the vertical. Note that the mean emission time will not be a good representation if the minimum and maximum emission times in the (space-time) averaging volume are significantly different. However, the high vertical resolution of the NAME simulations (200 m) and high temporal resolution (hourly) means that this uncertainty should be small. Figure 12a shows the mean emission time for ash particles over Chilbolton in the constant plume height simulation. It is assumed that although the NAME ash cloud arrives over Chilbolton 9 h earlier than observed, due to a small error in the position of the ash cloud moving southward over the UK, the time of the emission in the model is appropriate without any correction. Figure 12a shows that the upper part of the NAME ash cloud over Chilbolton was emitted, on average, between 00:00 and 06:00 UTC on 15 April. The sloping part of the ash cloud, which corresponds to the observations, was emitted earlier, on average between 18:00 UTC on 14 April and 00:00 UTC on 15 April. Thus if the plume height was overestimated between 00:00 and 06:00 UTC on 15 April as suggested by the Icelandic Meteorological Office radar measurements (Figure 1) this could have led to an overestimation of the ash cloud height at Chilbolton.

[37] Figure 12b shows the mean emission time for the constant plume height NAME simulated ash particles over Leipzig. Ash emitted in separate 6-h intervals extends in coherent sloped layers from 6 km down to 1 km. It is interesting that what appears as a single ash cloud over

Leipzig actually has complex structure when viewed in this manner. As for Chilbolton, ash near the surface was released at an earlier time than ash aloft. Comparison of the Chilbolton and Leipzig emission times shows that the ash emitted after 06:00 UTC on 15 April contributes to Leipzig but not to Chilbolton. Thus it is hypothesized that after 09:00 UTC on 15 April, during the period for which there were few radar observations, the plume height increased significantly from the 6 km value estimated to apply before 09:00 UTC to something closer to the 8.5 km value used in section 5.

6.4. High Plume Height Reconstruction

[38] Figure 13a shows the mass concentration over Leipzig for the high plume height reconstruction simulation. The upper layer of ash is captured by the NAME simulation as well as the early arrival of the ash cloud at 09:00 UTC. For quantitative agreement with the lidar column loadings the distal fine ash fraction is 4%. The comparison between NAME and Chilbolton lidar (not shown) is very similar to Figure 10a, as both the low and high plume height reconstructions have plume height ≤6 km between 00:00 and 09:00 UTC on 15 April compared to the constant plume height of 8.5 km.

7. Discussion and Conclusions

[39] The Eyjafjallajökull volcano in Iceland started to emit high concentrations of ash into the atmosphere on 14 April 2010. Ash emitted by the volcano was transported toward Europe and was observed by lidars at Reading, Cardington, Exeter, and Chilbolton in England and Leipzig in Germany on 16 April 2010. The UK Met Office dispersion model (NAME) has been used to simulate the evolution of the volcanic ash cloud and results have been compared to lidar
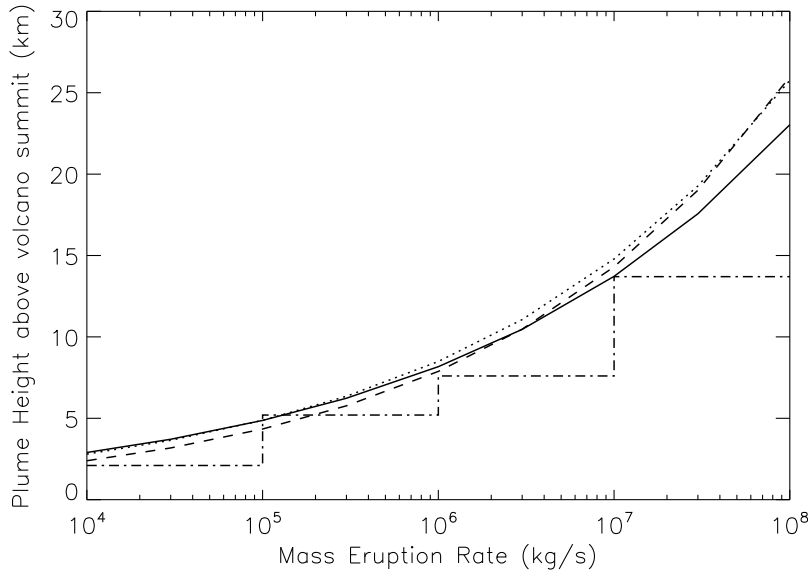
Figure A1. The variation of eruption rate with plume height used in NAME, $H = 0365M^{0.225}$ (solid line); *Mastin et al.* [2009], $H = 0.304M^{0.241}$ (dotted line); *Sparks et al.* [1997], $H = 0.220M^{0.259}$ (dashed line); and the emission rates from the NOAA VAFTAD thresholds (dash-dotted line).

observations. Leipzig was close to the central axis of the ash cloud, while the UK lidars were to the west of it. The transport of ash over the UK appears to have been parallel to a front associated with a low-pressure system centered to the north of Scandinavia.

[40] The accuracy of the NAME simulations depends on the accuracy of driving meteorological fields and volcano source parameters such as the plume height. The Icelandic radar observational data, used as plume height input, is mostly missing for an 18 h period during the initial phase of the eruption. In this paper NAME simulations have been compared to lidar observations made at Chilbolton and Leipzig using three different plume height input reconstructions.

[41] Taken together the Leipzig and Chilbolton observations are consistent with NAME if the volcanic plume height input represents the large variations on timescales of order 6 h in the plume height. These variations are broadly consistent with the Icelandic radar data. As a word of caution, using Chilbolton (or all of the UK lidars) only to perform the comparison would have given an ambiguous estimation of plume height. Model and observation comparisons are needed over a wide area, encompassing different parts of the ash cloud in order to give a reliable reconstruction. These results highlight the danger of using single observations to assess the performance of models in complex meteorological situations. They also show that it is necessary to accurately represent variations in emission height to produce accurate predictions. Therefore it matters how we cope with missing data, even for short periods.

[42] Overall, NAME appears to capture both the timing and vertical structure of the ash near the central axis of the ash cloud. Relatively small errors in the plume position, probably caused by the cumulative effect of errors in the driving meteorology en route, result in a timing error at distances far from the central axis of the ash cloud. Taking the timing error into account, NAME is able to capture the sloped ash layer over the UK. Quantitative comparison with the observed mass concentrations at Chilbolton and Leipzig suggests that around 3% of the total emitted mass is transported over long distances by small (<100 μm diameter) ash particles.

[43] Further work is desirable to investigate the meteorological timing error using ensemble meteorological analysis fields. Further work is also needed for later periods of the eruption to constrain further estimates of the distal fine ash fraction and to determine the sensitivity of this number to the assumed particle size distribution and the vertical distribution of ash at the source. A detailed study of the near field plume behavior, particularly for weak plumes involving strong interactions with the background atmosphere, would be beneficial for future volcanic eruptions.

Appendix A: Mass Eruption Rate

[44] In this paper the relationship relating the observed maximum plume height to the eruption rate is given by

$$H = 0.365M^{0.225}, \qquad (A1)$$

where H (km) is plume height above volcano summit and M (kg/s) represents the total mass eruption rate. The power law in this empirical relationship is based on a fit to a look-up table constructed by the National Oceanic and Atmospheric Administration (NOAA) for the VAFTAD (Volcanic Ash Forecast Transport and Dispersion) model [*Heffter and Stunder*, 1993] and reproduced by *Leadbetter and Hort* [2011]. The table gives threshold model concentrations in units/m^3 to be used with a model releasing a nominal 1 unit over the duration of a relatively short (<24 h) eruption in order to determine the extent of visual ash. It is intended for use with deep-layer averaged model concentrations (over depths of order 20,000 ft) and for use as a default value, to be modified in the light of satellite evidence. This threshold depends on both summit height and plume

height but here we have restricted consideration to a summit height equal to that of Eyjafjallajökull. At the London VAAC it was interpreted as relating to a release rate of 1 unit/6 h. Interpreting the threshold as inversely proportional to the actual emission rate means that the table can be interpreted as giving the shape of the M(H) function. The table gives a step function with changes in threshold (or source strength) in factors of 10 but a smooth power law was fitted through the data. The prefactor was then determined by comparing the values to the best fit curve given by *Mastin et al.* [2009]. Both in fitting the power law and determining the prefactor, the VAFTAD step function was regarded as most reliable at the top of each plume height range, and so only these values were used. This is based on the assumption that it was designed to ensure safety, and safety at the top of each height range implies that the safety margin at the bottom of each height range is larger than necessary. Figure A1 shows how equation (A1) relates to the empirical relationships of *Mastin et al.* [2009] and *Sparks et al.* [1997] and the emission rates estimated from the NOAA VAFTAD thresholds. The VAFTAD table was used by the London VAAC up until the eruption of Eyjafjallajökull and is used by the Washington VAAC. Equation (A1) was developed by the London VAAC during the eruption of Eyjafjallajökull.

References

Ansmann, A., et al. (2010), The 16 April 2010 major volcanic ash plume over central Europe: EARLINET lidar and AERONET photometer observations at Leipzig an Munich, Germany. *Geophys. Res. Lett.*, *37*, L13810, doi:10.1029/2010GL043809.

Arason, P., G. N. Petersen, and H. Bjornsson (2011), Observations of the altitude of the volcanic plume during the eruption of Eyjafjallajökull, April–May 2010, *Earth Syst. Sci. Data Discuss.*, *4*, 1–25, doi:10.5194/essdd-4-1-2011.

Bonadonna, C., and B. F. Houghton (2005), Total grain-size distribution and volume of tephra-fall deposits, *Bull. Volcanol.*, *67*, 441–456, doi:10.1007/s00445-004-0386-2

Bonadonna, C., G. Macedonio, and R. Sparks (2002), Numerical modelling of tephra fallout associated with dome collapses and Vulcanian explosions: Application to hazard assessment on Montserrat, in *The Eruption of Soufrière Hills Volcano, Montserrat, From 1995 to 1999*, edited by T. Druitt and B. Kokelaar, pp. 517–537, Geol. Soc. of London, London.

Casadevall, T. J. (1994), The 1989–1990 eruption of Redoubt volcano, Alaska: Impacts on aircraft operations, *J. Volcanol. Geotherm. Res.*, *62*, 301–316.

Clarisse, L., D. Hurtmans, A. J. Prata, F. Karagulian, C. Clerbaux, M. D.-Maziere, and P.-F. Coheur (2010a), Retrieving radius, concentration, optical depth, and mass of different types of aerosols from high-resolution infrared nadir spectra, *Appl. Opt.*, *49*, 3713–3722, doi:10.1364/AO.49.003713

Clarisse, L., F. Prata, J.-L. Lacour, D. Hurtmans, C. Clerbaux, and P.-F. Coheur (2010b), A correlation method for volcanic ash detection using hyperspectral infrared measurements, *Geophys. Res. Lett.*, *37*, L19806, doi:10.1029/2010GL044828.

Durant, A. J., W. I. Rose, A. M. Sarna-Wojcicki, S. Carey, and A. C. M. Volentik (2009), Hydrometeor-enhanced tephra sedimentation: Constraints from the 18 May 1980 eruption of Mount St. Helens, *J. Geophys. Res.*, *114*, B03204, doi:10.1029/2008JB005756.

Folch, A., A. Costa, A. Durant, and G. Macedonio (2010), A model for wet aggregation of ash particles in volcanic plumes and clouds: II. Model application, *J. Geophys. Res.*, *115*, B09202, doi:10.1029/2009JB007176.

Gangale, G., A. J. Prata, and L. Clarisse (2010), The infrared spectral signature of volcanic ash determined from high-spectral resolution satellite measurements, *Remote Sens. Environ.*, *114*, 414–425, doi:10.1016/j.rse.2009.09.007.

Guffanti, M., T. J. Casadevall, and K. Budding (2010), Encounters of aircraft with volcanic ash clouds; A compilation of known incidents, 1953–2009, *Data Ser. 545*, U.S. Geol. Surv., Reston, Va. (Available at http://pubs.usgs.gov/ds/545.)

Harrison, R. G., K. A. Nicoll, Z. Ulanowski, and T. A. Mather (2010), Self-charging of the Eyjafjallajökull volcanic ash plume. *Environ. Res. Lett.*, *5*, 024004, doi:10.1088/1748-9326/5/2/024004.

Heffter, J. L., and B. J. B. Stunder (1993), Volcanic Ash Forecast Transport And Dispersion (VAFTAD) model, *Weather Forecast.*, *8*, 534–541.

Hobbs, P. V., L. F. Radke, J. H. Lyons, R. J. Ferek, and D. J. Coffman (1991), Airborne measurements of particle and gas emissions from the 1990 volcanic eruptions of Mount Redoubt, *J. Geophys. Res.*, *96*, 18,735–18,752.

Holasek, R. E., and W. I. Rose (1991), Anatomy of 1986 Augustine volcano eruptions as recorded by multispectral image processing of digital AVHRR weather satellite data, *Bull. Volcanol.*, *53*, 420–435.

James, M. R., J. S. Gilbert, and S. J. Lane (2002), Experimental investigation of volcanic particle aggregation in the absence of a liquid phase, *J. Geophys. Res.*, *107*(B9), 2191, doi:10.1029/2001JB000950.

Jones, A., D. Thomson, M. Hort, and B. Devenish (2007), The UK Met Office's next-generation atmospheric dispersion model, NAME III, in *Air Pollution Modeling and its Application XVII*, edited by C. Borrego and A-L. Norman, pp. 580–589, Springer, New York.

Leadbetter, S. J., and M. C. Hort (2011), Volcanic ash hazard climatology for an eruption of Hekla Volcano, Iceland, *J. Volcanol. Geotherm. Res.*, *199*, 230–241.

Maryon, R. H., D. B. Ryall, and A. L. Malcolm (1999), The NAME 4 dispersion model: Science documentation, *Met Off. Turbulence and Diffus. Note 262*, Natl. Meteorol. Libr., Exeter, U. K.

Mastin, L. G., et al. (2009), A multidisciplinary effort to assign realistic source parameters to moels of volcanic ash-cloud transport and dispersion during eruptions, *J. Volcanol. Geotherm. Res.*, *186*, 10–21.

Rose, W. I., G. J. S. Bluth, and G. G. J. Ernst (2000), Integrating retrievals of volcanic cloud characteristics from satellite remote sensors: A summary, *Philos. Trans.*, *358*, 1585–1606.

Schneider, D. J., and W. I. Rose (1994), Observations of the 1989–90 Redoubt Volcano eruption clouds using AVHRR satellite imagery, *U.S. Geol. Surv. Bull.*, *2047*, 405–418.

Sparks, R. S. J., M. Bursik, S. N. Carey, J. A. Gilbert, L. S. Glaze, H. Sigurdsson, and A. W. Woods (1997), *Volcanic Plumes*, John Wiley, Chichester, U. K.

Webley, P. W., B. J. B. Stunder, and K. G. Dean (2009), Significant eruption source parameter(s) for operational ash cloud transport and dispersion models, *J. Volcanol. Geotherm. Res.*, *186*, 108–119.

Webster, H. N., and D. J. Thomson (2008), Dry deposition modelling in a Lagrangian dispersion model, paper presented at 12th Conference on Harmonisation Within Atmospheric Dispersion Modelling for Regulatory Purposes, Meteorol. and Hydrol. Serv. of Croatia, Cavtat, Croatia.

Wilson, L., R. Sparks, T. Huang, and N. Watkins (1978), The control of volcanic column heights by eruption energetics and dynamics, *J. Geophys. Res.*, *83*, 1829–1836.

Witham, C. S., M. C. Hort, R. Potts, R. Sevranckx, P. Husson, and F. Bonnardot (2007). Comparison of VAAC atmospheric dispersion models using the 1 November 2004 Grimsvotn eruption, *Meteorol. Appl.*, *14*, 27–38.

A. Ansmann and I. Mattis, Leibniz Institute for Tropospheric Research, Permoserstrasse 15, D-04318 Leipzig, Germany.

S. E. Belcher, H. F. Dacre, A. L. M. Grant, and R. J. Hogan, Department of Meteorology, University of Reading, Earley Gate, PO Box 243, Reading, RG6 6BB, UK. (h.f.dacre@reading.ac.uk)

L. Clarisse, Spectroscopie de l'Atmosphère, Service de Chimie Quantique et Photophysique, Université Libre de Bruxelles, B-1050 Brussels, Belgium.

B. J. Devenish, J. M. Haywood, M. C. Hort, F. Marenco, and D. J. Thomson, Met Office, FitzRoy Road, Exeter EX1 3PB, UK.